communications earth & environment

Article

https://doi.org/10.1038/s43247-024-01737-5

Natural forest regeneration is projected to reduce local temperatures

Check for updates

Sara Alibakhshi[1,2] ✉, Susan C. Cook-Patton[3], Edouard Davin[4,5,6], Eduardo Eiji Maeda[1,7], Miguel Bastos Araújo[8,9,10], Daniel Heinlein[11], Janne Heiskanen[1,7], Petri Pellikka[1,12,13] & Thomas W. Crowther[2]

Forest regeneration is a crucial strategy for mitigating and adapting to global warming. Yet its precise impact on local climate remains uncertain, a factor that complicates decision-making when it comes to prioritizing investments. Here, we developed global maps illustrating how natural forest regeneration influences key local climate drivers—land surface temperature (LST), albedo, and evapotranspiration—using models fitted at a 1-km spatial resolution with a random forest classifier. We found that natural forest regeneration can alter annual mean LST by 0.01 °C, −0.59 °C, −0.50 °C, and −2.03 °C in Boreal, Mediterranean, Temperate, and Tropical regions, respectively. These variations underscore the region-specific effects of forest regeneration. Importantly, natural forest regeneration reduces LST across 64% of 1 billion hectares and 75% of 148 million hectares of potentially restorable land under different scenarios. These findings improve understanding of how forest regeneration can help regulate local climate, supporting climate adaptation efforts.

Efforts to mitigate climate change and adapt to its impact often highlight forest regeneration as one of the key strategies[1–3]. Forest regeneration plans garnered significant scientific attention in recent years[4–6], with a debate emerging on the efficacy of such initiatives[7–9], the temperature impacts of forests[10], and the choice of high-priority areas for regeneration[11] (see supplementary text S2.2). Despite the ongoing scientific debate on the merits of forest regeneration as a policy response to climate change, several governmental, non-governmental, and private sector organizations are already promoting forest regeneration programs all over the world. This highlights the urgent need for a robust understanding of how strategic implementation of forest regeneration can offer adaptation benefits.

Forests can have impacts beyond just climate mitigation. Specifically, two major biophysical factors modified by forests that contribute to shaping local climatic conditions are land surface albedo (whereby plants change the reflectivity of the land surface) and evapotranspiration (whereby plants release water to the atmosphere)[12–17]. Trees tend to be optically darker than open lands and snow, thus increasing tree cover has the potential to lower albedo, leading to increased absorption of solar radiation[17]. This, along with other factors, may contribute to local climate warming in certain regions[18,19]. Such warming effects can be potentially offset if the absorbed solar radiation is redistributed through increasing evapotranspiration which is an energy-intensive process[20]. Albedo and evapotranspiration (ET) can vary significantly across regions[21,22] due to different environmental conditions (i.e., soil characteristics, vegetation types, snow conditions, and atmospheric humidity[23–25], and their interplay will ultimately control local land surface temperature (LST).

Given the rising frequency of extreme heat events[26] and their impacts on the living world[27], it is increasingly critical to understand where forest regeneration is likely to have warming or cooling impacts to facilitate decision-making around climate-related targets. Here, we employed machine learning models to produce the 1-km maps of changes in LST, albedo, and evapotranspiration following natural forest regeneration. Natural forest regeneration refers here to the spontaneous or assisted recovery of diverse mixtures of native tree species in an area where a forest ecosystem

[1]Department of Geosciences and Geography, University of Helsinki, Helsinki, Finland. [2]Institute of Integrative Biology, ETH Zürich, Zürich, Switzerland. [3]The Nature Conservancy, Arlington, VA, USA. [4]Wyss Academy for Nature, University of Bern, Bern, Switzerland. [5]Climate and Environmental Physics, Physics Institute, University of Bern, Bern, Switzerland. [6]Oeschger Centre for Climate Change Research, University of Bern, Bern, Switzerland. [7]Finnish Meteorological Institute, Helsinki, Finland. [8]Department of Biogeography and Global Change, National Museum of Natural Sciences, CSIC, Madrid, Spain. [9]Rui Nabeiro Biodiversity Chair, MED – Mediterranean Institute for Agriculture, Environment and Development & CHANGE – Global Change and Sustainability Institute, University of Évora, Évora, Portugal. [10]Theoretical Sciences Visiting Program, Okinawa Institute of Science and Technology Graduate University, Onna, Japan. [11]Graduate School and Research, Arcada University of Applied Sciences, Helsinki, Finland. [12]State Key Laboratory of Information Engineering in Surveying, Mapping and Remote Sensing, Wuhan University, Wuhan, PR China. [13]University of Nairobi, Wangari Maathai Institute for Environmental and Peace Studies, P.O. Box 29053 - 00625, Kangemi, Kenya. ✉e-mail: sara.alibakhshi@gmail.com

was previously disturbed or depleted[28,29]. While previous studies have focused on historical data to uncover the impact of forests on local temperatures at coarse resolution[30,31], we examine the effect of increases in forest cover to provide spatially explicit information for future climate change adaptation policies.

Results

We examined the relationship between a suite of explanatory variables (e.g., climate and soil variables, see supplementary text, S1.1) and response variables (LST, albedo, and evapotranspiration) in intact forests. We used this information to create a wall-to-wall model to predict potential LST (°C), albedo (dimensionless), and evapotranspiration (kg/m²/time) in locations potentially suitable for regenerating natural forests (Figs. 1 and 2 and supplementary figs. S2–S7). We identified ~1 billion hectares where natural forest regeneration is theoretically feasible, which is a 'less conservative scenario'. To generate this area, we excluded regions unequivocally unsuitable for forest regeneration—such as water bodies, existing forests, urban areas[32], and regions identified as nonviable for forest regrowth[33]. In a 'more conservative scenario', we identified close to 148 million hectares suitable for natural forest regeneration. This was based on the opportunity map by Griscom et al.[3], which considers areas that are critical for food security and biodiversity conservation. We further excluded urban areas, and any areas classified as nonviable for forest regrowth[33]. The boundaries of these areas are illustrated in Fig. 1A for the more conservative scenario and in supplementary fig. S2 for the less conservative scenario. For both scenarios, we then computed ΔLST, Δalbedo, and ΔET, which represent the annual mean differences between predicted values following the regeneration and observed values in the potential areas to mitigate the effects of residuals (supplementary text S1.2.2).

Our results indicate that in the less conservative scenario, ~709 million hectares, representing 64.19% of the potential area, could experience a reduction in LST with an annual median value decrease of 0.37 °C. In contrast, the more conservative scenario anticipates that 75.15% of the much smaller potential area, ~111 million hectares, would experience cooling, with a more substantial annual median temperature reduction of 1.46 °C following natural forest regeneration.

The extent of cooling varies substantially across different regions. For instance, in the less conservative scenario, our model predicts warming rather than cooling in 87% of the potential area in the Boreal region, whereas in Tropical regions, only 9% might see ΔLST increases. The polar bar plot showed the distribution of various land use classes in areas identified as potential sites for natural forest regeneration under the more conservative scenario (Fig. 1C). The robustness of these predictions has been validated

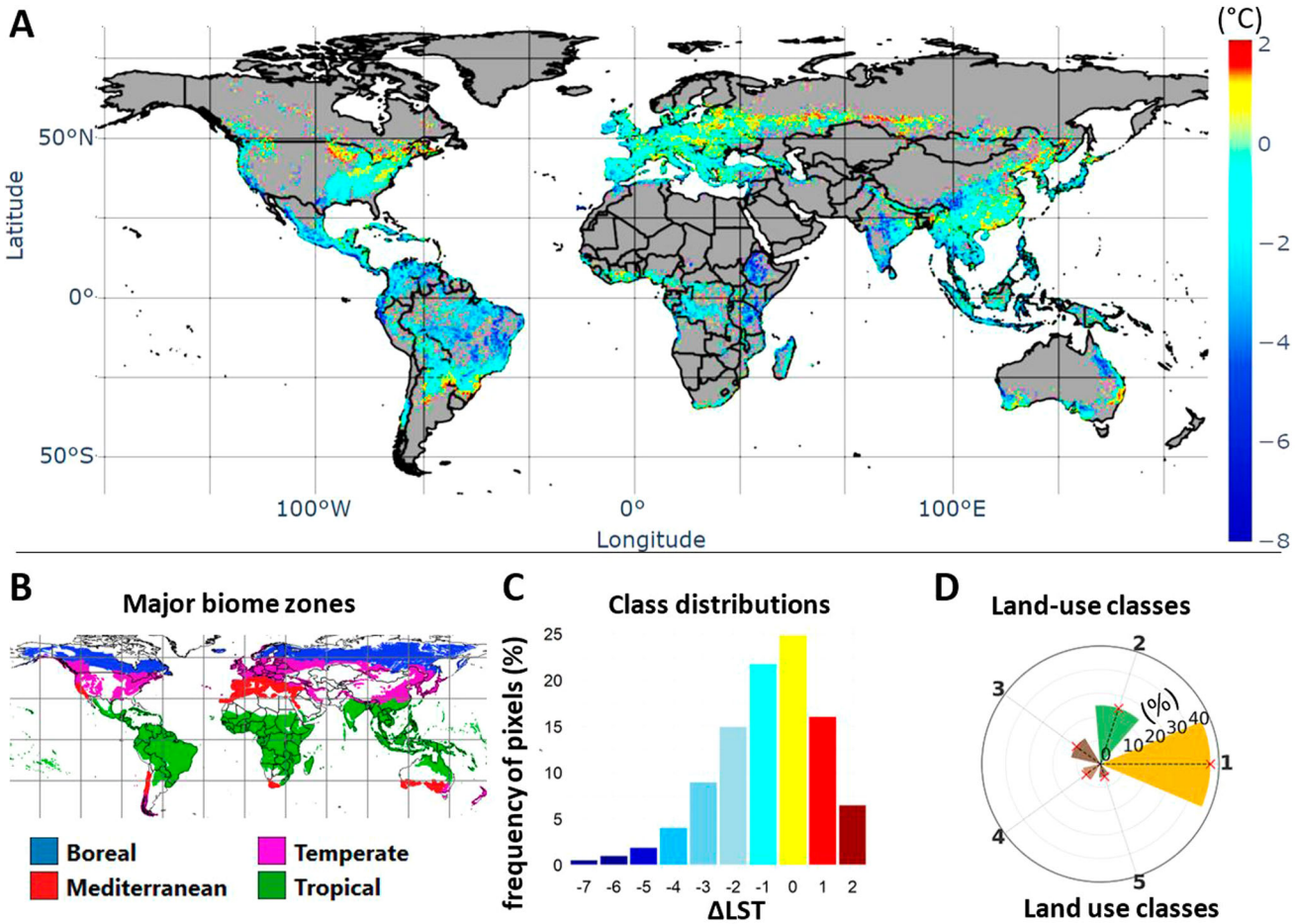

Fig. 1 | Predicted change in land surface temperature (ΔLST) following natural forest regeneration. A This figure illustrates the expected variation in ΔLST (°C), calculated as the difference between the predicted LST after forest regeneration and the currently observed LST. The analysis focuses on regions identified as having restoration potential and presents data at a 1-km spatial resolution. **B** Location of major biome zones, including Boreal, Mediterranean, Temperate, and Tropical regions. **C** Class distributions of predicted change in ΔLST, where the y-axis represents the percentage distribution of pixel frequencies across a range of values from −8 to 2 and a label i on the x-axis represents the interval [i-1 °C, i °C[of ΔLST values. **D**. Land use classes in potential areas for natural forest regeneration. Class 1 (savanna: 46.37%), class 2 (grassland: 24.77%), class 3 (croplands, 12.46%), class 4 (cropland/natural vegetation mosaic: 7.52%), and class 5 (Woody Savannas, 5.63%); other classes (<4%) are not depicted in the figure. In both **A** and **C**, red colors indicate places where natural regeneration would lead to local warming, blue colors indicate cooling, and yellow indicates no change.

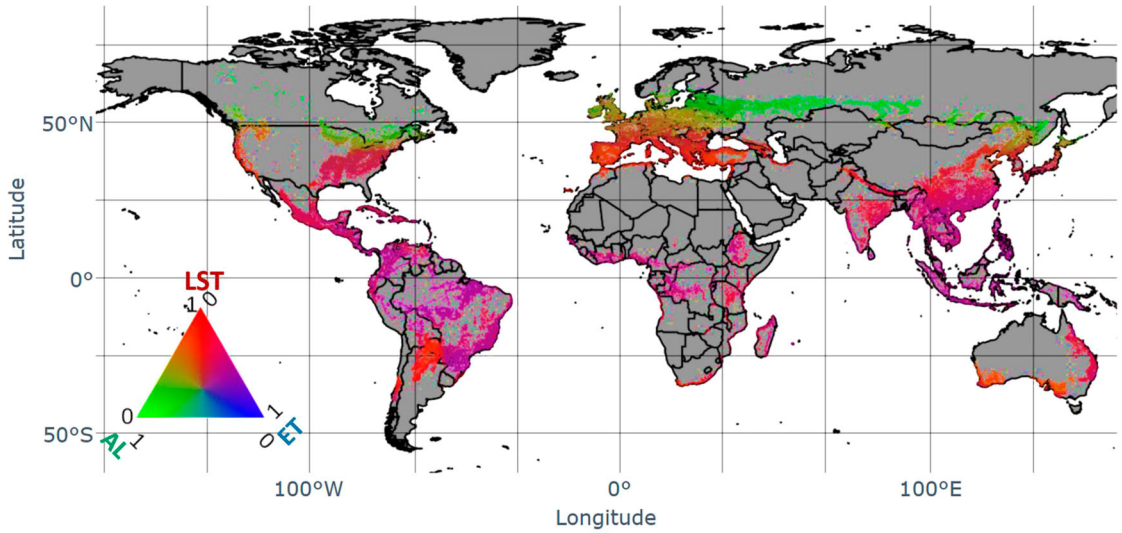

Fig. 2 | Relationship between modeled land surface temperature (LST), land surface albedo (AL), and evapotranspiration (ET) following natural forest regeneration. The predictions are provided at a 1-km spatial resolution identified for forest regeneration. LST (°C) is represented with increased gradients of red; albedo (dimensionless) is represented with increased gradients of green; and evapotranspiration (kg/m^2/time) is represented with increased gradients of blue. The gray color represents the background color. The accompanying legend employs a ternary plot where each axis reflects the proportional influence of LST, AL, and ET, ranging from 0% to 100%. The color composition within any given pixel on the map corresponds to the combined influence of these variables, which collectively add up to 100%. For example, purple pixels near Hong Kong suggest an approximate equal influence (ca. 50%) from both LST and ET, with a negligible contribution from AL. While 100% LST is red, 100% AL is blue, and 100% ET is green, the rotation of 0 and 1 of the axes labelings contains the information on how to decode any color in the ternary plot.

using 5-fold cross-validation, as documented in the supplementary text (S1.2.2) and presented in supplementary tables S1–S6.

In general, the Boreal region is the least likely to experience cooling as the result of natural forest regeneration, with an average increase in annual mean ΔLST of 0.04 °C under the more conservative scenario and an annual mean increase of 8.83 °C under the less conservative scenarios (supplementary tables S1 and S4. respectively). This warming trend in the Boreal region appears to be primarily attributable to changes in albedo (Fig. 2., supplementary fig. S3.), which is shown to have the highest decreases in Δalbedo across all examined regions (supplementary table S2.). On the other hand, the Mediterranean, Temperate, and Tropical regions generally exhibit a cooling trend with natural forest regeneration. Under the more conservative scenario, our results suggest that natural forest regeneration could result in annual mean ΔLST reductions of 1.59 °C in the Mediterranean, 0.50 °C in the Temperate, and 2.03 °C in the Tropical regions (supplementary table. S1). This cooling effect is even more pronounced under the less conservative scenario, with annual mean ΔLST reductions of 1.41 °C, 0.39 °C, and 3.25 °C for the Mediterranean, Temperate, and Tropical regions, respectively (supplementary table. S4). The Tropical region showed the greatest degree of cooling, consistent with previous studies[34–36]. In general, places with reductions in LST, all featured increases in ΔET (supplementary table S3), alongside modest declines in Δalbedo (supplementary table S2, Fig. 2, and supplementary fig. S3).

In the more conservative scenario, the maximum cooling effect (i.e., highest annual median observed reduction in LST) could reach an annual median change of 4.18 °C in the Boreal, −6.37 °C in the Mediterranean, −4.93 °C in the Temperate, and −6.37 °C in the Tropical regions following natural forest regeneration. In contrast, we observe maximum ΔLST could reach up to an annual median warming of 4.28 °C in the Boreal, 4.94 °C in the Mediterranean, 4.12 °C in the Temperate, and 2.29 °C in the Tropical regions. The areas destined to warm exhibited average decreases in Δalbedo and smaller rises in ΔET when compared to areas expected to cool (supplementary tables S1–S6).

To further test the robustness of our models, we compared predicted values in LST, albedo, and evapotranspiration with observed data in recently regenerated areas. We first identified areas with global tree gains, subsequently filtering out regions with artificially planted trees, namely afforested areas[37], and excluding patches <3600 m^2. This refinement process yielded a total focus area of 353,505 hectares. The performance of our models was good, as evidenced by the coefficient of determination (R^2 values) for LST, albedo, and evapotranspiration, which were 0.87, 0.47, and 0.76, respectively, indicating a substantial alignment with observed data (Fig. 3.).

Discussion

This study provides the global map of LST, albedo, and evapotranspiration variation following natural forest regeneration at 1-km spatial resolution, examining two scenarios: one less conservative, covering approximately a billion hectares, and another more conservative, covering around 148 million hectares. Opportunity for local cooling after regeneration of forests is substantial, with about 64.19% of the areas in the first scenario and 75.15% in the second scenario, witnessing an annual median LST reduction of 0.37 °C and 1.46 °C, respectively. The variation in LST underscores the importance of identifying and critically selecting apt regions for forest regeneration initiatives[38,39]. This variability suggests that substantial temperature modulation—either cooling or warming—can occur even within a single biome, thereby highlighting the value of detailed maps such as ours in identifying areas that yield maximal climate cooling benefits. For example, within the northernmost areas of the Boreal biome in North America (Fig. 1A), targeted natural regeneration could result in localized cooling, corroborating previous empirical findings[30]. The cooling effect of forests in some regions such as Boreal can be attributed to factors such as forest structure, forest composition, geographical location of forests, snow quantity and quality, and their varying impacts on the reflectivity of the land[40,41].

There are large global forest restoration ambitions, which are primarily focused on rapid biodiversity and climate mitigation[42]. Yet, our analysis indicates that ~36% of the potential one billion hectares available for natural forest regeneration would increase LST. Balancing climate mitigation and adaptation efforts in the forest restoration plans is crucial. Failing to address the tradeoff between maximizing carbon storage and potential local temperature changes may inadvertently lead to unintended consequences. For example, the ΔLST post-natural forest regeneration can hit the maximum

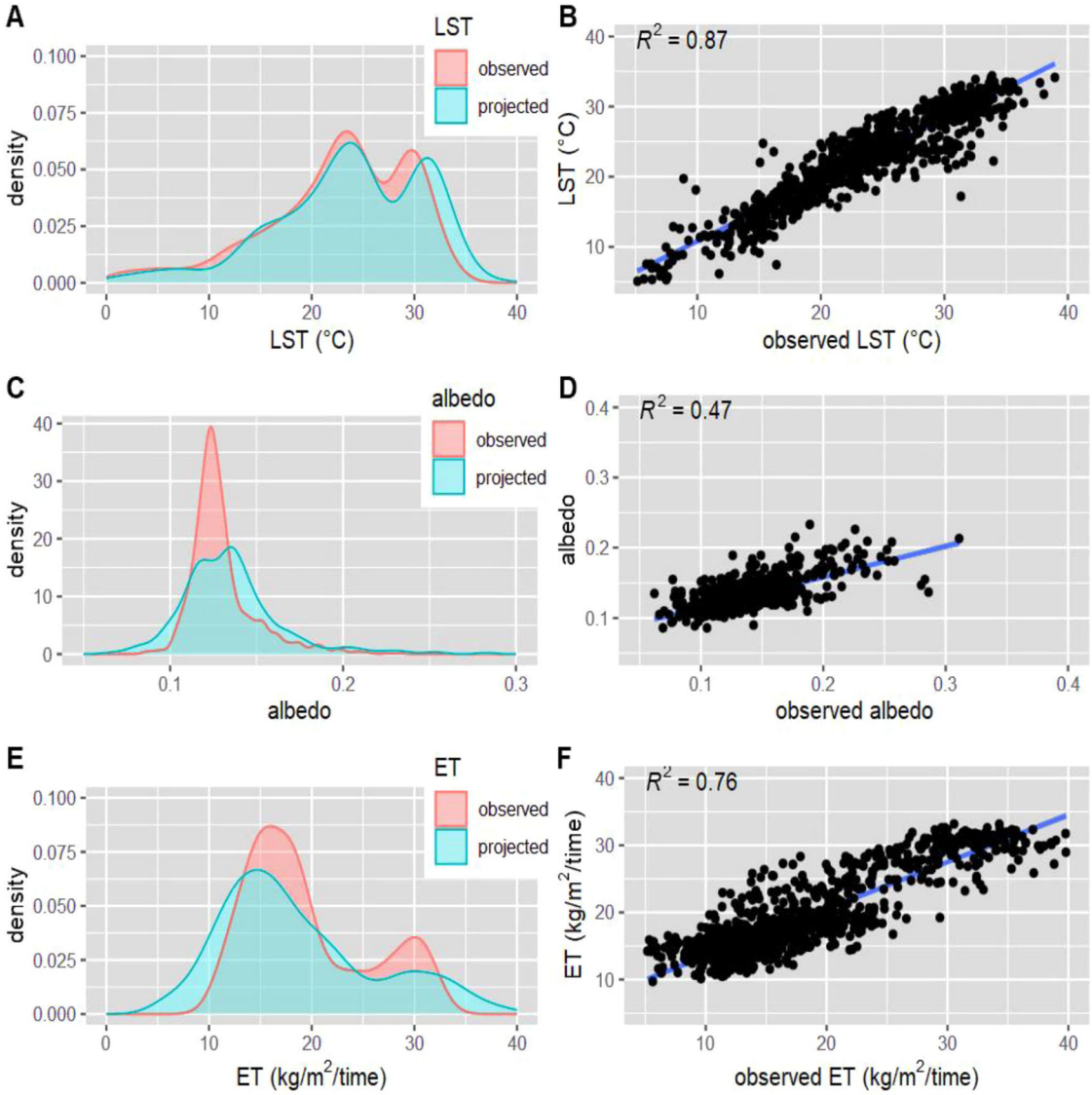

Fig. 3 | Model validation for predicting changes in land surface temperature (LST), albedo, and evapotranspiration (ET) following natural forest regeneration. Panels **A**, **C**, and **E** present density plots contrasting observed and predicted values of LST (°C), albedo (dimensionless), and evapotranspiration (kg/m^2/time), respectively, within areas that have undergone regeneration. Panels **B**, **D**, and **F** illustrate the relationship between the actual measurement of LST, albedo, and evapotranspiration from forests (plotted on the x-axes) and the corresponding predicted values derived from our models (plotted on the y-axes).

value of 4.94 °C, which increases the potential risk to thermal habitat suitability of certain species, human wellbeing, and ecosystem services. Strategic planning combined with informed participatory decision-making are essential to ensure that forest restoration initiatives not only enhance carbon sequestration but also contribute to local climate resilience.

This study provides a much finer spatial resolution of 1-km spatial resolution relative to the ca. 111-km spatial resolution in earlier studies[14,30,31]. We were also able to substantially improve predictions of changes in LST compared to previous studies (e.g., see reference number *31*), which reported an R^2 of 0.34. The improvement in our analysis stems from the methodology employed in our study (supplementary text S1.2), which forgoes the conventional rolling window searches over time and space that were prevalent in prior studies[30,31]. In addition, our models include a larger range of environmental predictors—including soil characteristics—that were overlooked in previous studies. Soil types differ in their heat capacity, moisture retention, and thermal conductivity, all of which affect heat exchange processes between the Earth's surface and the atmosphere, thereby impacting local temperature dynamics[43,44].

The Boreal region is less likely to experience cooling due to forest regeneration, with some areas even experiencing local warming (Fig. 1A and supplementary table. S1). This local warming trend is primarily attributed to changes in albedo which can lead to higher absorption of solar radiation[14–17,25]. However, the models have the weakest prediction power for the Boreal region (supplementary table S1), and the validation for predicting changes in albedo performed poorly (Fig. 3). The albedo component remains less reliable, likely using annual mean values rather than seasonal variations in albedo, which do not account for significant snow-related changes that influence albedo seasonally in the Boreal region. Such uncertainties complicate decision-making for forest regeneration projects in Boreal regions.

The identified areas for potential forest regeneration (Fig. 1A) encompass current land use classes, including grassland and savannas (Fig. 1C), posing challenges for conversion to forests due to presence of established ecosystems and competing land use interests (see supplementary text S2.2). Furthermore, the Food and Agriculture Organization of the United Nations (FAO) reported that between 2010 and 2020, the annual net

forest area change was -4.7 million hectares, with over 90 percent of the world's forests regenerating naturally[45]. This highlights the challenge of regenerating between 111 million and 709 million hectares of forests, depending on the scenario. Despite these difficulties, regenerating forests is crucial for effective climate mitigation. Griscom et al. [3] emphasized that natural climate solutions, such as forest regeneration, could provide over one-third of the cost-effective climate mitigation required by 2030 to limit global warming to below 2 °C. In addition, Cook-Patton et al. [46] highlighted that natural forest regrowth can significantly contribute to climate stabilization by mid-century[46]. While modeling the air temperature benefit of current forests can help to inform climate policy recommendations, this study focused on modeling LST associated with natural forest regeneration plans. LST is particularly valuable because it directly reflects the temperature of the land surface, which is influenced by factors such as vegetation, soil, and moisture levels. This allows LST to present crucial temperature-dependent physiological processes and energy exchanges occurring within the vegetated canopy[47].

Although the potential of forest regeneration to cool down the local climate is promising (supplementary table S1), the available land associated with a local cooling effect for such efforts is limited to 7.15% of the total global land area in the less conservative scenario and 1.12% of the total global land area in the more conservative scenario (supplementary text S2.1)[48]. Further, ultimately only a fraction of this land may be restorable, given competing land use demands[49]. Therefore, our study highlights the need for deploying a combination of multiple solutions, both nature-based and gray infrastructure solutions for climate mitigation and adaptation, with a focus on "no regrets" strategies that deliver benefits regardless of future climate outcomes[50]. It is the case of well-designed and carefully implemented natural forest regeneration, which brings multiple environmental and ecological benefits, as forests play a critical role in regulating carbon[21,51,52], water cycle, and biodiversity preservation[53–55]. Recognizing that it is impractical to regenerate forests universally, our work is crucial in prioritizing areas where forest regeneration will have the positive impact on climate adaptation. We stress that the primary motivation for forest regeneration should be the local well-being of people and the biodiversity that they depend on[56]. With the growing threat of widespread deforestation on our planet's ecosystems, our findings highlight the crucial role of the urgent need for natural forest conservation and regeneration in supporting climate resilience at the local level.

Materials and methods

In this study, we employed a data-driven machine learning algorithm called random forest model[57,58] to assess variation in LST[59], albedo[60], and evapotranspiration[61] within existing forests to predict these variables in areas globally that lack forest cover but have the potential for natural forest regeneration. Data-driven approaches such as random forest based on direct observations from satellite data can improve estimates of the biogeophysical characteristics of forests by addressing the inherent uncertainties in process-based models relevant to our study[62–64]. Such approaches can account for the confounding effects of multiple variables influencing biogeophysical processes across diverse environmental conditions by capturing the non-linear and complex relationships between these variables and the resulting patterns (Supplementary Text S.1).

We used variable importance analysis and multicollinearity test to determine the key variables for explaining response variables, i.e., LST, albedo, and evapotranspiration, to be served as predictor variables for model development and optimization by using only the most relevant and independent variables (supplementary text S1.1)[65]. We selected a set of explanatory variables which mainly present the geo-environmental parameters such as slope, elevation, aspect, soil properties, topographic information, incoming solar radiation, distance to road, and climate zones (supplementary text S1.1). The predictor variables do not include any direct information on the forest characteristics (e.g., Leaf Area Index (LAI), canopy cover). By excluding direct information which characterize forests, the model can better predict LST, albedo, and evapotranspiration, resembling species distribution models. In other words, the strategic selection of training variables enables accurate prediction in diverse landscapes. To extract training data, we first identified stable forests through trend analyses using Theil-Sen's slope, removing any pixels that showed a significant decline (p-value: 0.05) in the LAI (supplementary text S1.2.1). Having a consistent spatial database, we aggregated all the datasets to a 1-km spatial resolution using the mean function for all the predictors and response variables, except for the land cover map that was aggregated with a modal function. Following the extraction of datasets from stable forest locations, we addressed varying missing values in response variables per year during the study period, using a two-step process between 2003 and 2021. First, we calculated the mean values of LST, albedo, and evapotranspiration for each pixel for each calendar month, creating 12 monthly maps. Then, we computed the overall mean LST, albedo, and evapotranspiration for each pixel by averaging these monthly means across between 2003 and 2021 (supplementary text S1.2.1).

Two scenarios were analyzed to assess the potential impacts of natural forest regeneration: a less conservative scenario identifying ~1 billion hectares suitable for natural forest regeneration, and a more conservative scenario focusing on 148 million hectares, accounting for food security and biodiversity constraints. The less conservative scenario excluded existing forests, and urban regions and nonviable areas such as water bodies. In contrast, the more conservative scenario further constrained the suitable areas based on the opportunity map by Griscom et al. [3], emphasizing regions critical for food security and biodiversity conservation. We delineated the boundaries of Boreal, Mediterranean, Temperate, and Tropical forests were based on an ecoregion map[66], which provides a spatial classification of distinct ecological zones according to bioclimatic, vegetation, and geographical criteria (supplementary fig. S1.1). Next, we built four random forest models over Boreal, Mediterranean, Temperate, and Tropical forests to predict LST, albedo, and evapotranspiration for each scenario. In each model, we used over 25,000 random points and validated the results using 20% of the sample points which were never used to develop the random forest model. By using bootstrap aggregating, or so-called bagging, which is a machine learning ensemble meta-algorithm, we minimized the risk of overfitting. The robustness of these predictions was validated using 5-fold cross-validation (see Supplementary Text S1.2.1 and Tables S1–S6). Additionally, we tested the models by comparing predicted LST, albedo, and evapotranspiration with observed data in recently regenerated areas (Figs. 3, S1.2.1, and S1.2.2).

After predicting LST, albedo, and evapotranspiration across potential areas following natural forest regeneration, we quantified the changes in these variables resulting from the regeneration process. The window searching technique is a widely used remote sensing method for quantifying the biogeophysical impact of forests compared with non-forest areas. It employs a spatial window—such as ~50 km × 28 km in Li et al. (2015) and 111 km × 111 km in Bright et al. [14]—to evaluate the differences in biogeophysical characteristics between forests and non-forestlands or stable forests. However, the method may introduce uncertainties in certain regions such as the Amazonian forests, where finding pure open lands close to dense forests is challenging. In addition, with a such large spatial window, environmental factors such as soil type, annual precipitation, proximity to water bodies, and distance to urban areas can vary significantly, potentially leading to errors in estimating the temperature benefits of forests. At a coarse spatial resolution, the results of different forest patches within a coarse pixel might cancel out each other. Furthermore, the results may not be interpretable due to different land types within a single pixel. Hence, we quantified impact of natural forest regeneration on the LST, albedo, and evapotranspiration (ΔLST, Δalbedo, Δ evapotranspiration, respectively) via:

$$\Delta LST = LST_{predicted\ forest} - LST_{observed\ values\ in\ potential\ area} \quad (1)$$

$$\Delta albedo = albedo_{predicted\ forest} - albedo_{observed\ values\ in\ potential\ area} \quad (2)$$

$$\Delta ET = ET_{predicted\ forest} - ET_{observed\ values\ in\ potential\ area} \quad (3)$$

This formula allows us to remove the residual signal due to climate variability and isolate the cooling effect of the forest by removing the baseline temperature of potential areas, which may be influenced by residual signals from local climate variability and noise. Positive values of ΔLST indicate warming effects due to the natural forest regenerations, while negative values indicate cooling.

We showed the interplay between LST, albedo, and evapotranspiration through a global map depicted in Fig. 2. The color scheme in the map is derived from a ternary plot, serving as the legend. The ternary plot employs barycentric coordinates to represent the three variables, LST, albedo, and evapotranspiration. In the ternary plot, we have rescaled the values of each pixel such that the sum of LST, albedo, and evapotranspiration equals 100%. This rescaling enables us to represent the three variables in a two-dimensional format, simplifying the intricate compositional relationships between LST, albedo, and evapotranspiration and simplifying the complex compositional relationships between the variables. Let X be a 2-dimentional matrix. Define:

$$m(X) = \min_{i,j} X_{i,j} \quad (4)$$

$$M(X) = \max_{i,j} X_{i,j} \quad (5)$$

and the 2-dimensional matrix $S(X)$ defined entry-wise by:

$$S(X)_{i,j} = \frac{X_{i,j} - m(X)}{M(X) - m(X)} \quad (6)$$

The proportions adding to 100% and determining the color via the ternary diagram are then calculated as:

$$\frac{S(LST)_{i,j}}{S(LST)_{i,j} + S(Albedo)_{i,j} + S(ET)_{i,j}} \quad (7)$$

$$\frac{S(Albedo)_{i,j}}{S(LST)_{i,j} + S(Albedo)_{i,j} + S(ET)_{i,j}} \quad (8)$$

$$\frac{S(ET)_{i,j}}{S(LST)_{i,j} + S(Albedo)_{i,j} + S(ET)_{i,j}} \quad (9)$$

More details on modeling the consequence of forest regeneration plans on LST, albedo, and evapotranspiration can be found in the supplementary material file, including the plots of predicted change in LST, albedo, and evapotranspiration following natural forest regeneration (supplementary figs. S2–S7).

Data availability

The MODIS land surface temperature (LST) data, including MYD11A1 and MOD11A1, as well as albedo (MCD43A1), evapotranspiration (MOD16A2) data and global leaf area index (LAI) data (MCD15A3H), can be accessed via NASA's Earth Observing System Data and Information System (EOSDIS) at https://earthdata.nasa.gov. The Global Roads Inventory Project (GRIP4) data can be accessed at https://www.globio.info, and soil data from SoilGrids and WoSIS are available at https://soilgrids.org/. The WorldClim dataset for solar radiation can be found at https://www.worldclim.org. More information on data related to this study can be found: https://doi.org/10.5281/zenodo.13766638.

Code availability

All code and functions used in this study were executed using the built-in functions and APIs provided by Google Earth Engine (GEE). For example, the random forest model used in this study can be found here. Custom Python 3 code was developed specifically for data visualization, which can be found: https://zenodo.org/records/13769609.

Received: 1 March 2024; Accepted: 27 September 2024;
Published online: 10 October 2024

References

1. Nolan, C. J., Field, C. B. & Mach, K. J. Constraints and enablers for increasing carbon storage in the terrestrial biosphere. *Nat. Rev. Earth Environ.* **2**, 436–446 (2021).
2. Domke, G. M., Oswalt, S. N., Walters, B. F. & Morin, R. S. Tree planting has the potential to increase carbon sequestration capacity of forests in the United States. *Proc. Natl Acad. Sci. USA* **117**, 24649–24651 (2020).
3. Griscom, B. W. et al. Natural climate solutions. *Proc. Natl Acad. Sci. USA* **114**, 11645–11650 (2017).
4. Lefebvre, D. et al. Assessing the carbon capture potential of a reforestation project. *Sci. Rep.* **11**, 19907 (2021).
5. Busch, J. et al. Potential for low-cost carbon dioxide removal through tropical reforestation. *Nat. Clim. Change* **9**, 463–466 (2019).
6. Tuinenburg, O. A., Bosmans, J. H. & Staal, A. The global potential of forest restoration for drought mitigation. *Environ. Res. Lett.* **17**, 034045 (2022).
7. Roebroek, C. T., Duveiller, G., Seneviratne, S. I., Davin, E. L. & Cescatti, A. Releasing global forests from human management: How much more carbon could be stored? *Science* **380**, 749–753 (2023).
8. Seddon, N., Turner, B., Berry, P., Chausson, A. & Girardin, C. A. Grounding nature-based climate solutions in sound biodiversity science. *Nat. Clim. Change* **9**, 84–87 (2019).
9. Naudts, K. et al. Forest management: Europe's forest management did not mitigate climate warming. *Science* **351**, 597–599 (2016).
10. Arora, V. K. & Montenegro, A. Small temperature benefits provided by realistic afforestation efforts. *Nat. Geosci.* **4**, 514–518 (2011).
11. Windisch, M. G., Davin, E. L. & Seneviratne, S. I. Prioritizing forestation based on biogeochemical and local biogeophysical impacts. *Nat. Clim. Change* **11**, 867–871 (2021).
12. Le Quéré, C. et al. Global carbon budget 2014. *Earth Syst. Sci. Data* **7**, 47–85 (2015).
13. O'Halloran, T. L. et al. Radiative forcing of natural forest disturbances. *Glob. Change Biol.* **18**, 555–565 (2012).
14. Bright, R. M. et al. Local temperature response to land cover and management change driven by non-radiative processes. *Nat. Clim. Change* **7**, 296–302 (2017).
15. Bonan, G. B., Pollard, D. & Thompson, S. L. Effects of boreal forest vegetation on global climate. *Nature* **359**, 716–718 (1992).
16. Bright, R. M. et al. Climate change implications of shifting forest management strategy in a boreal forest ecosystem of Norway. *Glob. Change Biol.* **20**, 607–621 (2014).
17. Bright, R. M., Zhao, K., Jackson, R. B. & Cherubini, F. Quantifying surface albedo and other direct biogeophysical climate forcings of forestry activities. *Glob. Change Biol.* **21**, 3246–3266 (2015).
18. Betts, R. A. Offset of the potential carbon sink from boreal forestation by decreases in surface albedo. *Nature* **408**, 187–190 (2000).
19. Davin, E. L. & de Noblet-Ducoudre, N. Climatic impact of global-scale Deforestation: radiative versus nonradiative processes. *J. Clim.* **23**, 97–112 (2010).
20. Ban-Weiss, G. A., Bala, G., Cao, L., Pongratz, J. & Caldeira, K. Climate forcing and response to idealized changes in surface latent and sensible heat. *Environ. Res. Lett.* **6**, 034032 (2011).
21. Bonan, G. B. Forests and climate change: forcings, feedbacks, and the climate benefits of forests. *Science* **320**, 1444–1449 (2008).
22. Alibakhshi, S., Naimi, B. Hovi, A., Crowther, T. W. & Rautiainen, M. Quantitative analysis of the links between forest structure and land surface albedo on a global scale. *Remote Sens. Environ.* **246**, 111854 (2020).

23. Su, Z. The surface energy balance system (SEBS) for estimation of turbulent heat fluxes. *Hydrol. Earth Syst. Sci.* **6**, 85–99 (2002).
24. Bastiaanssen, W. G., Menenti, M., Feddes, R. & Holtslag, A. A remote sensing surface energy balance algorithm for land (SEBAL). 1. Formulation. *J. Hydrol.* **212**, 198–212 (1998).
25. Bright, R. M. et al. Inferring surface albedo prediction error linked to forest structure at high latitudes. *J. Geophys. Res.: Atmos.* **123**, 4910–4925 (2018).
26. Horton, R. M., Mankin, J. S., Lesk, C., Coffel, E. & Raymond, C. A review of recent advances in research on extreme heat events. *Curr. Clim. Change Rep.* **2**, 242–259 (2016).
27. González-Trujillo, J. D., Román-Cuesta, R. M., Muñiz-Castillo, A. I., Amaral, C. H. & Araújo, M. B. Multiple dimensions of extreme weather events and their impacts on biodiversity. *Clim. Change* **176**, 155 (2023).
28. Chazdon, R. L. & Guariguata, M. R. Natural regeneration as a tool for large-scale forest restoration in the tropics: prospects and challenges. *Biotropica* **48**, 716–730 (2016).
29. Crouzeilles, R. et al. Ecological restoration success is higher for natural regeneration than for active restoration in tropical forests. *Sci. Adv.* **3**, e1701345 (2017).
30. Alkama, R. & Cescatti, A. Climate change: biophysical climate impacts of recent changes in global forest cover. *Science* **351**, 600–604 (2016).
31. Li, Y. et al. Local cooling and warming effects of forests based on satellite observations. *Nat. Commun.* **6**, 6603–6603 (2015).
32. Friedl, M. & Sulla-Menashe, D. MCD12Q1 MODIS/Terra+ aqua land cover type yearly L3 global 500m SIN grid V061. *NASA EOSDIS Land Process. DAAC* **10**, 200 (2022).
33. Bastin, J.-F. et al. The global tree restoration potential. *Science* **365**, 76–79 (2019).
34. Li, Y. et al. Potential and actual impacts of deforestation and afforestation on land surface temperature. *J. Geophys. Res.: Atmos.* **121**, 14,372–314,386 (2016).
35. Zeppetello, L. R. V. et al. Consistent cooling benefits of silvopasture in the tropics. *Nat. Commun.* **13**, 708 (2022).
36. Windisch, M. G., Davin, E. L., & Seneviratne, S. I. Prioritizing forestation based on biogeochemical and local biogeophysical impacts. *Nat. Clim. Change* **11**, 867–871 (2021).
37. Harris, N., Goldman, E. D. & Gibbes, S. Spatial database of planted trees (SDPT) version 1.0. *Technical Note, World Resources Institute* (2019).
38. Crouzeilles, R. et al. Achieving cost-effective landscape-scale forest restoration through targeted natural regeneration. *Conserv. Lett.* **13**, e12709 (2020).
39. Chazdon, R. L. & Uriarte, M. Natural regeneration in the context of large-scale forest and landscape restoration in the tropics. *Biotropica* **48**, 709–715 (2016).
40. Kuusinen, N., Tomppo, E. & Berninger, F. Linear unmixing of MODIS albedo composites to infer subpixel land cover type albedos. *Int. J. Appl. Earth Observation Geoinf.* **23**, 324–333 (2013).
41. Hovi, A. et al. Seasonal dynamics of albedo across European boreal forests: Analysis of MODIS albedo and structural metrics from airborne LiDAR. *Remote Sens. Environ.* **224**, 365–381 (2019).
42. Rayden, T., Jones, K. R., Austin, K. & Radachowsky, J. Improving climate and biodiversity outcomes through restoration of forest integrity. *Conserv. Biol.* **37**, e14163 (2023).
43. Abu-Hamdeh, N. H. Thermal properties of soils as affected by density and water content. *Biosyst. Eng.* **86**, 97–102 (2003).
44. Dai, Y. et al. Evaluation of soil thermal conductivity schemes for use in land surface modeling. *J. Adv. Model. Earth Syst.* **11**, 3454–3473 (2019).
45. Food and Agriculture Organization of the United Nations. (2020). *Global Forest Resources Assessment 2020: Main report*. https://openknowledge.fao.org/server/api/core/bitstreams/9f24d451-2e56-4ae2-8a4a-1bc511f5e60e/content. Date of access: 20 May 2024
46. Cook-Patton, S. C. et al. Mapping carbon accumulation potential from global natural forest regrowth. *Nature* **585**, 545–550 (2020).
47. Mildrexler, D. J., Zhao, M. & Running, S. W. A global comparison between station air temperatures and MODIS land surface temperatures reveals the cooling role of forests. *J. Geophys. Res. Biogeosci.* **116**, G03025 (2011).
48. Li, Y. et al. Green spaces provide substantial but unequal urban cooling globally. *Nat. Commun.* **15**, 7108 (2024).
49. Araújo, M. B. & Alagador, D. Expanding European protected areas through rewilding. *Curr. Biol.* **34**, 3931–3940.e5 (2024).
50. Paterson, J. S., Araújo, M. B., Berry, P. M., Piper, J. M. & Rounsevell, M. D. A. Mitigation, adaptation, and the threat to biodiversity. *Conserv. Biol.* **22**, 1352–1355 (2008).
51. Bustamante, M. M. et al. Ecological restoration as a strategy for mitigating and adapting to climate change: Lessons and challenges from Brazil. *Mitig. Adapt. Strateg. Glob. Change* **24**, 1249–1270 (2019).
52. Richter, D. D., Markewitz, D., Trumbore, S. E. & Wells, C. G. Rapid accumulation and turnover of soil carbon in a re-establishing forest. *Nature* **400**, 56–58 (1999).
53. Canadell, J. G. & Raupach, M. R. Managing forests for climate change mitigation. *Science* **320**, 1456–1457 (2008).
54. Staal, A. et al. Forest-rainfall cascades buffer against drought across the Amazon. *Nat. Clim. Change* **8**, 539–543 (2018).
55. Spracklen, D. V., Arnold, S. R. & Taylor, C. Observations of increased tropical rainfall preceded by air passage over forests. *Nature* **489**, 282–285 (2012).
56. Erbaugh, J. et al. Global forest restoration and the importance of prioritizing local communities. *Nat. Ecol. Evol.* **4**, 1472–1476 (2020).
57. Liaw, A. & Wiener, M. Classification and regression by randomForest. *R News* **2**, 18–22 (2002).
58. Breiman, L. Random forests. *Mach. Learn.* **45**, 5–32 (2001).
59. Wan, Z., Hook, S. & Hulley, G. MOD11A2 MODIS/Terra Land Surface Temperature/Emissivity 8-Day L3 Global 1km SIN Grid V006. *NASA EOSDIS Land Processes DAAC*, **10** (2015).
60. Schaaf, C., Wang, Z., Schaaf, C. & Wang, Z. MCD43A1 MODIS/Terra+ Aqua BRDF/albedo model parameters daily L3 global–500 m V006. EOSDIS L. Process. DAAC, NASA, Washington, DC, USA, *Tech. Rep*. (2015).
61. Running, S., Mu, Q. & Zhao, M. Mod16A2 modis/terra net evapotranspiration 8-day l4 global 500m sin grid v006. *NASA EOSDIS Land Processes DAAC*, **6** (2017).
62. Perugini, L. et al. Biophysical effects on temperature and precipitation due to land cover change. *Environ. Res. Lett.* **12**, 053002 (2017).
63. Pitman, A. J. et al. Uncertainties in climate responses to past land cover change: first results from the LUCID intercomparison study. *Geophys. Res. Lett.* **36**, L14814 (2009).
64. Sonntag, S., Pongratz, J., Reick, C. H. & Schmidt, H. Reforestation in a high-CO2 world—Higher mitigation potential than expected, lower adaptation potential than hoped for. *Geophys. Res. Lett.* **43**, 6546–6553 (2016).
65. Naimi, B., Hamm, N. A. S., Groen, T. A., Skidmore, A. K. & Toxopeus, A. G. Where is positional uncertainty a problem for species distribution modelling? *Ecography* **37**, 191–203 (2014).
66. Olson, D. M. et al. Terrestrial ecoregions of the world: a new map of life on earth: a new global map of terrestrial ecoregions provides an innovative tool for conserving biodiversity. *Bioscience* **51**, 933–938 (2001).

Acknowledgements

We would like to thank the institutions and individuals who contributed to this research. We thank the MODIS project for providing access to essential land surface temperature (LST) data, as well as other datasets like albedo, evapotranspiration, and leaf area index through NASA's Earth Observing System Data and Information System (EOSDIS). Special thanks to the

Finnish Research Impact Foundation for supporting this research. We would like to acknowledge the use of Google Earth Engine for providing the computational platform and satellite data processing tools used in this research. This research was supported by the Finnish Research Impact Foundation. The Bezos Earth Fund supported SCP's time on this work. Research by MBA was partly conducted while visiting the Okinawa Institute of Science and Technology (OIST) through the Theoretical Sciences Visiting Program (TSVP). Open access funded by Helsinki University Library.

Author contributions

In the conceptualization phase, Prof. Thomas W Crowther and Sara Alibakhshi jointly formulated the foundational idea. Sara Alibakhshi led the study and conducted the analyses. The valuable contributions of Susan C. Cook-Patton significantly improved the draft. Edouard Davin and Eduardo Eiji Maeda made significant contributions by proposing new analyses that enhanced the presentation and interpretation of the results. Miguel Bastos Araújo, Daniel Heinlein, Janne Heiskanen, and Petri Pellikka contributed to refining the writing and offering constructive comments and feedback throughout the process.

Competing interests

The authors declare no competing interests.

Additional information

Supplementary information The online version contains supplementary material available at https://doi.org/10.1038/s43247-024-01737-5.

Correspondence and requests for materials should be addressed to Sara Alibakhshi.

Peer review information *Communications Earth and Environment* thanks Katia Fernandes, Lisa Biber-Freudenberger for their contribution to the peer review of this work. Primary Handling Editors: Paula Prist and Martina Grecequet, Aliénor Lavergne. A peer review file is available.